

Quantum dot based ultrafast photoconductive antennae for efficient THz radiation

Andrei Gorodetsky, Natalia Bazieva, and Edik U. Rafailov

Optoelectronics and Biomedical Photonics Group, Aston Institute of Photonic Technologies,
Aston University, Birmingham, B4 7ET, UK

ABSTRACT

Here we overview our work on quantum dot based THz photoconductive antennae, capable of being pumped at very high optical intensities of higher than 1 W optical mean power, i.e. about 50 times higher than the conventional LT-GaAs based antennae. Apart from high thermal tolerance, defect-free GaAs crystal layers in an InAs:GaAs quantum dot structure allow high carrier mobility and ultrashort photocarrier lifetimes simultaneously. Thus, they combine the advantages and lacking the disadvantages of GaAs and LT-GaAs, which are the most popular materials so far, and thus can be used for both CW and pulsed THz generation. By changing quantum dot size, composition, density of dots and number of quantum dot layers, the optoelectronic properties of the overall structure can be set over a reasonable range - compact semiconductor pump lasers that operate at wavelengths in the region of 1.0 μm to 1.3 μm can be used. InAs:GaAs quantum dot-based antennae samples show no saturation in pulsed THz generation for all average pump powers up to 1 W focussed into 30 μm spot. Generated THz power is superlinearly proportional to laser pump power. The generated THz spectrum depends on antenna design and can cover from 150 GHz up to 1.5 THz.

Keywords: THz Generation, Quantum Dots, Photoconductive Antenna, Semiconductors

1. INTRODUCTION

Photoconductive antennae (PCA) for coherent THz signal generation and detection were successfully demonstrated for the first time in 1984.¹ Since that initial demonstration, there is still a great deal of research dedicated to the design of THz antennas in almost every aspect of such devices. Quantum dots (QD) were introduced shortly after the seminal work into photoconductive antennae in 1985² and since then have found themselves involved in many photonic applications, such as diode lasers,³⁻⁵ amplifiers,⁶ and saturable absorbers.⁷ All these applications take advantage of QD's high thermal and optoelectronic efficiency and short charge carrier lifetime.

Defect-free GaAs crystal layers in an InAs:GaAs quantum dot structure are responsible for high carrier mobility, and incorporated InAs QDs serve to shorten carrier lifetimes down to below 1 ps.⁷ Thus, QD wafer combines the the best properties of most widely used so far PCA substrate materials: high carrier mobility of GaAs and ultrashort carrier lifetimes of LT-GaAs. This unique properties combination opens up the ability to use QD-based antennae for both CW and pulsed THz generation. Moreover, semiconductor wafer engineering allows tuning of structure pump wavelength within a reasonable range, well beyond the GaAs energies, allowing to use compact and relatively cheap ultrafast semiconductor³ or fibre⁸ (for pulsed regime) and narrow line double-wavelength semiconductor⁴ or fibre⁹ pump lasers (for CW regime) that operate at wavelengths between 1.0 μm to 1.3 μm .

After seminal work on implementation of QD structures in compact and powerful semiconductor lasers, we decided to try them as photoconductive THz emitters, and during past three years confirmed their efficiency in both pulsed and CW regimes¹⁰⁻¹⁶ and proposed further actions that can be taken for ultimate system upgrade to achieve even more efficient THz generation in more compact environment. In this proceeding, we review and update all our results on THz generation with QD based PCAs.

Further author information: Send correspondence to E.U.R.

E-mail: e.rafailov@aston.ac.uk

2. ANTENNA DESIGN AND FABRICATION

2.1 QD wafers

We used InAs:GaAs QD structures and varied numbers of InAs QD layers therein (25 layers for Structure 25 and 40 layers for Structure 40 correspondingly). Structures were grown over a suitable distributed Bragg reflector (DBR) adjusted to work ideally for pump wavelengths. All semiconductor structures were grown by molecular beam epitaxy (MBE) in the Stranski-Krastanov regime, comprising a 30 nm top layer of LT-GaAs above an active QD layer region of either 25 or 40 layers of InAs QDs immediately beneath.

In all cases, the QD layers were each capped by 4 nm to 5 nm $\text{In}_{0.15}\text{Ga}_{0.85}\text{As}$ layer and separated by a 35 nm to 36 nm GaAs spacer layer, giving a total active region depth between 1 μm to 1.7 μm comprising either twenty-five or forty 40 nm QD sections. A TEM image of a single QD is shown in Figure 1(b). An extra spacer layer of GaAs was grown beneath the active PC region followed by an AlAs/GaAs DBR of either 25 or 30 layers (Figure 1(a)). Structures were grown by Innolume GmbH, Germany, and by the EPSRC National Centre for III-V Technologies at the University of Sheffield, UK. Growth parameters for the QD layers were intentionally kept as similar as possible between structures.

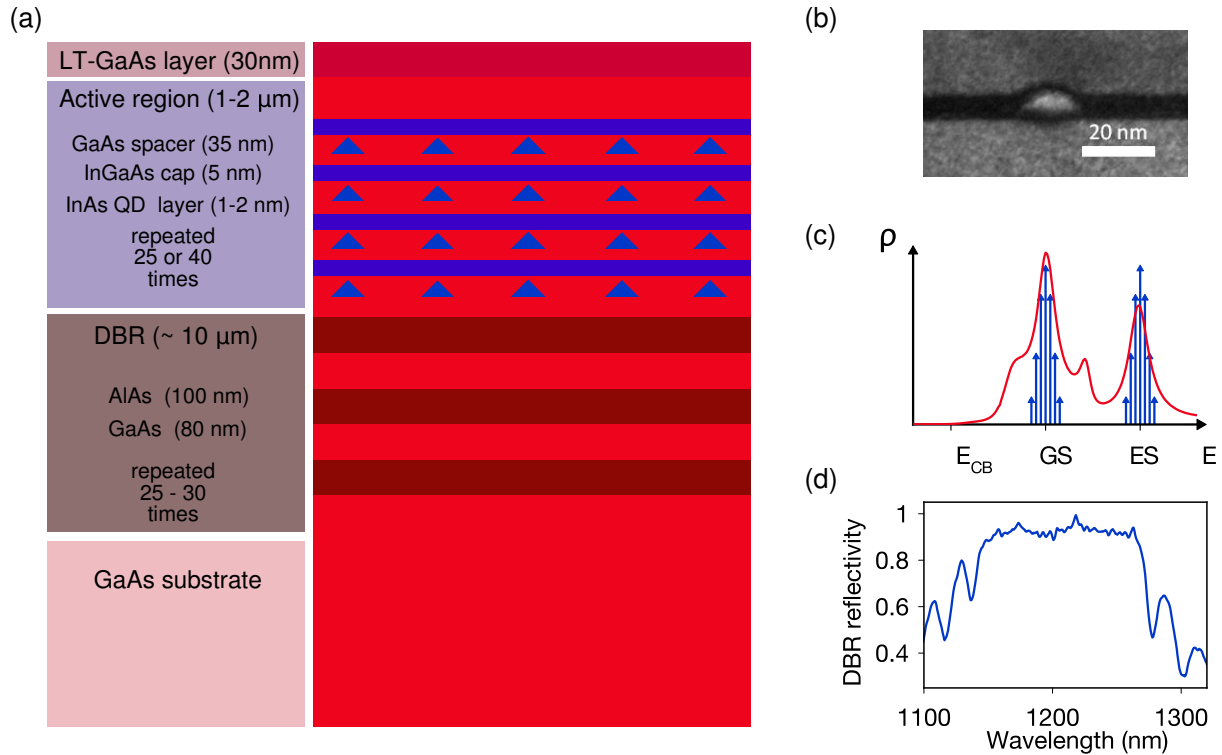


Figure 1. (a) Epitaxial layer profile of a QD wafer used for THz generation, (b) TEM image of a InAs QD inside GaAs lattice, (c) QD structure density of states (blue arrows) and its photoluminescence spectrum, (d) measured DBR reflectivity.

Ideal QDs demonstrate three dimensional carrier confinement, exhibiting discrete energy levels. However, in real QD structures the density of states (DOS) is smudged into a Gaussian-type distribution around each energy level due to variations in the deposited dot sizes (Figure 1(c)). The DBR is used to reflect pump IR radiation beam thus reducing the IR power at the antenna output, to re-use its power for extra pump and to allow intra-cavity operation in future. Typical measured DBR reflectivity of the samples used is shown in Figure 1(d).

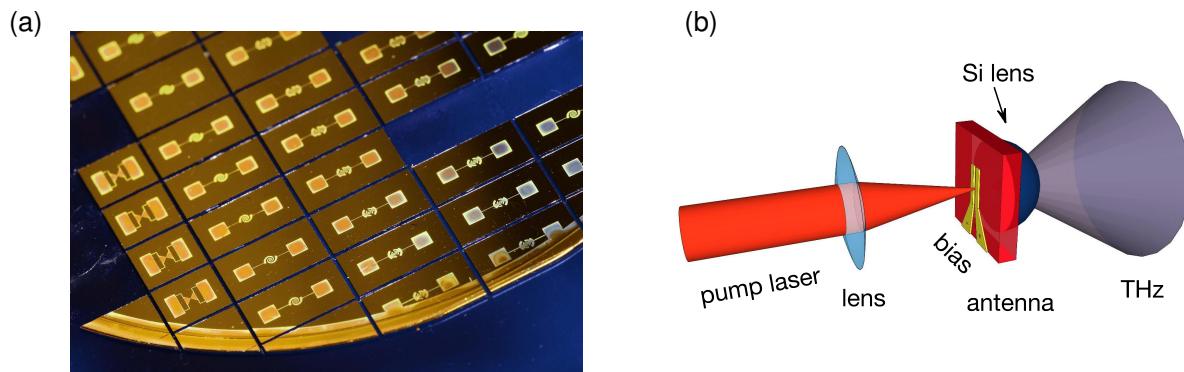


Figure 2. (a) Image of QD wafer with antenna electrodes, (b) PCA principle of operation.

2.2 Antenna layout, electrodes and outcoupling

Principle of PCA operation is well-known and exists for over 30 years:¹ radiation of ultrafast laser is collimated into the gap between antenna electrodes to generate photocarriers, and the latter are moved across with applied electric bias until they relax back to non-conducting state. Generated ultrafast current produces EM field of THz frequencies, excitation pulse duration and carrier lifetime define its spectral width. In CW photomixing regime, antenna is pumped with IR radiation of two closely spaced wavelengths (so that the frequency difference lies within THz range). Produced THz radiation is directed by PCA electrodes and additionally collimated with silicon lens that also serves as a heatsink (Fig. 2(b)).

Production of metallic microantennas over semiconductor substrate was done using standard UV photolithography, wet etching and a post-process anneal to increase Ohmic contact between antenna metal and GaAs surface. The contact metals were deposited in 25 nm Ti + 40 nm Pt + 100 nm Au ratio. Ti was used in to enable a high degree of metal-semiconductor adhesion and to prevent softer metal diffusion. Wafer with deposited antenna electrodes, variously shaped to match different operation regimes are shown in Fig. 2 (a).

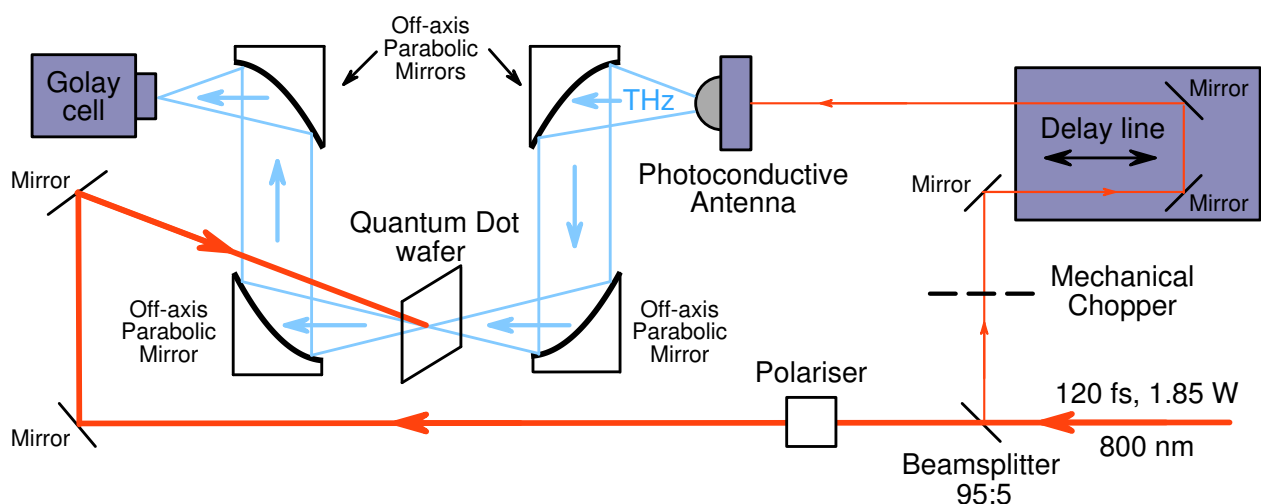


Figure 3. Experimental setup for IR-pump THz-probe measurements

3. QD WAFER LIFETIME EVALUATION

Semiconductor carrier lifetime is a crucial characteristic that defines its efficiency in pulsed regime. Earlier studies of QD wafer lifetimes^{7,17-20} have shown InAs QDs to shorten the carriers lifetime down to around or below 1 ps, regardless the lifetime evaluation technique involved: measurements were done in IR-pump – IR-probe,⁷ THz-pump – IR-probe¹⁹ and IR-pump – THz-probe.²⁰ Within the scope of our current research we estimated carriers lifetime using our IR pump - THz probe setup shown in Fig. 3.

The same optical source is used to induce the excess of carriers in the QD sample, as well as to gate the photoconductive transmitter antenna generating the THz probe beam. In our lab, we employ femtosecond Ti:sapphire laser (M Squared, model Sprite-XT) with pulse duration of 120 fs at 80 MHz repetition rate and 800 nm wavelength and average power of 1.8 W. A commercial LT-GaAs coplanar stripline PCA (TeraVil Ltd.) is used to generate the THz probe beam, which then propagates through a 4 off-axis parabolic mirrors system. Both the optical pump and the THz probe beams are focussed onto the same overlapping region of the sample (≈ 1 mm diameter). The THz signal transmitted through the QD structure is then focussed into a Golog cell detector (Tydex, model GC-1P) which in conjunction with a lock-in amplifier and a mechanical chopper allows to implement homodyne detection. The THz signal transmitted through the sample is then recorded for varying positions of the delay line, and for different optical pump intensities, obtained by means polariser placed in the pump beam.

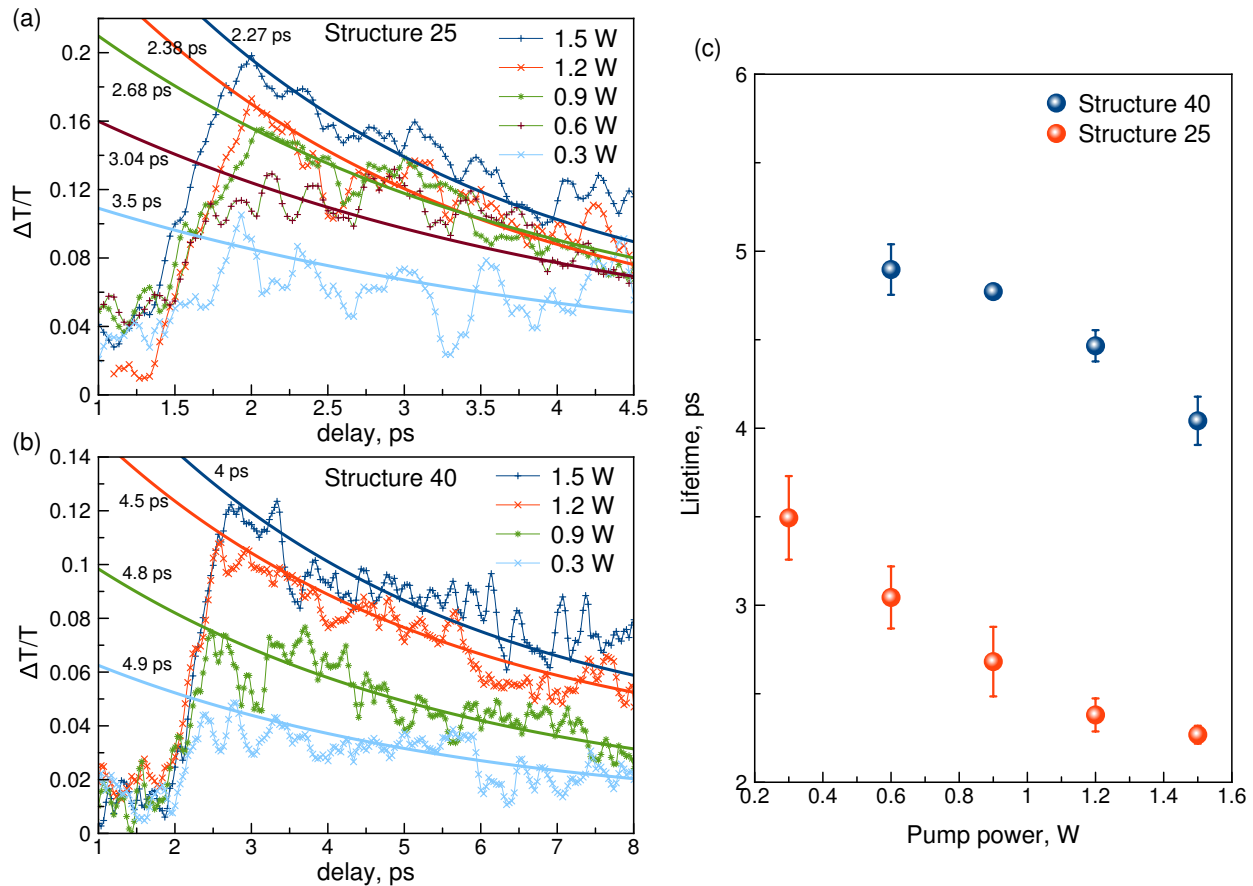


Figure 4. IR pump – THz probe measurements in QD wafers, (a) and (b) – relative transmission changes in Structure 25 and Structure 40 correspondingly, (c) – lifetime dependency on IR pump power.

When pumped at the wavelengths around 800 nm (allowing excitation of the GaAs barrier layers), radiative process timescales can range from one to hundreds of ps.¹⁸ These timescales are determined by generation and

diffusion of carriers from the GaAs into the QDs, simultaneous state-filling of QD energy levels, and subsequent energy-dependent exciton recombination. Importantly however, it is observed that an increasing optical pump power leads firstly to saturation of the dot ground state (GS) and subsequently of the higher energy states, that have shorter recombination time as compared to the GS.²¹

Our measurements also confirm these results, as we observe carrier lifetime shortening with the increasing IR pump power. Differential transmission curves and lifetime derived from exponential fit are shown in Fig. 4 (a) and (b) correspondingly. Lifetime drops from ~ 4 ps down to ~ 2 ps in Structure 25 and from ~ 5 ps down to ~ 4 ps in Structure 40 when the sample is pumped with 1.5 W average power. Thus, physical origin behind the observed spectral broadening in the emission of QD-based photoconductive transmitters with increasing pump power may indeed be the carrier lifetime shortening, confirming the hypothesis that under higher pumping intensities the carriers undergo non-radiative relaxation through QD excited states rather than through the slower ground states.

4. QD ANTENNA OFF-RESONANT HIGH-POWER PUMP OPERATION

Commercially available bow-tie LT-GaAs based PCA for THz generation usually have the power limit of 10 mW to 20 mW mean optical power at 50 MHz to 100 MHz repetition rate,²² i.e. 3000 W/cm^2 pump intensities. We show our QD photoconductive structures to operate under pump intensities of about 50 times higher, i.e. up to above 1 W, without saturation in the $I_{THz} \propto P_{pump}^2$ pump dependency in this range of laser powers. Measurement results for Bow-tie PCA over Structure 25 are shown in Fig. 5. As it can be seen, power of the generated THz radiation is quadratically proportional to both pump power, that exceeds 1 W, and antenna bias voltage.

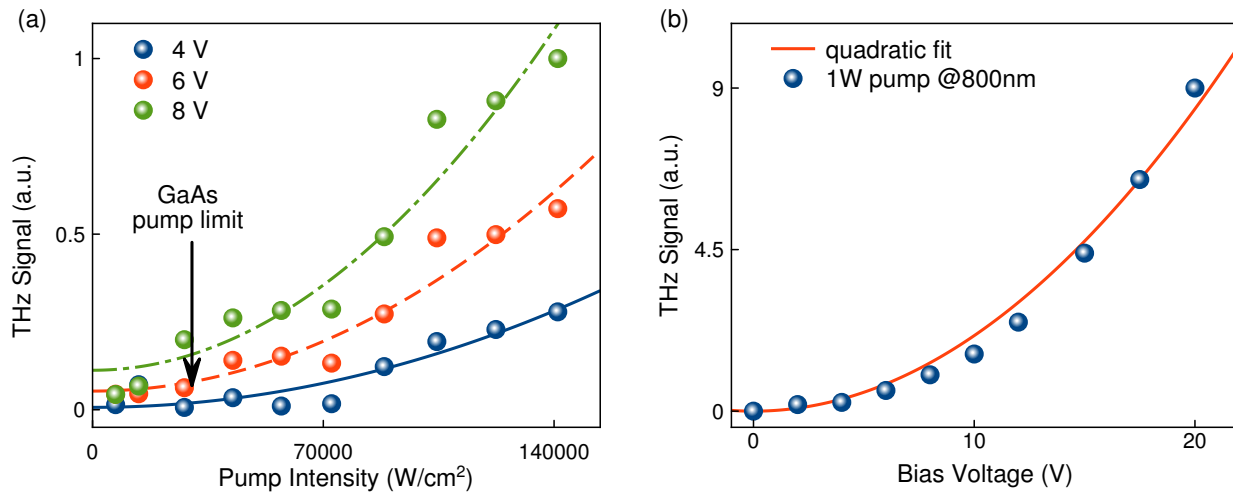


Figure 5. Operation of bow-tie QD-based PCA under off-resonant high-power pump of 800 nm. (a) Dependence of generated THz power on IR pump intensity, (b) dependence of generated THz power on bias applied to antenna electrodes.

To run coherent time-domain QD PCA characterisation, we employ our THz time-domain spectroscopic (THz-TDS) setup, but replace commercial LT GaAs PCA emitter with home brewed QD PCA and let significantly higher powers to engage it. In this case, we show results for log-periodic PCA with $8 \mu\text{m}$ photoconductive gap over Structure 25. We use previously described in section 3 fs pump laser and setup, depicted in Fig. 3, slightly modified for coherent detection with LT-GaAs THz PCA detector from Teravil.²³

Time-domain measurement results and corresponding spectra are shown in Fig. 6 (a) and (b) correspondingly.

Under higher pump powers, not only the amplitude of the main peak grows, but also its shortening can be clearly observed. Main peak FWHM change with pump power is plotted in the inset of Fig. 6 (a), and it halves from 1.65 ps to 0.8 ps within seven-fold rise of pump power from 100 mW to 700 mW. Fourier transformed

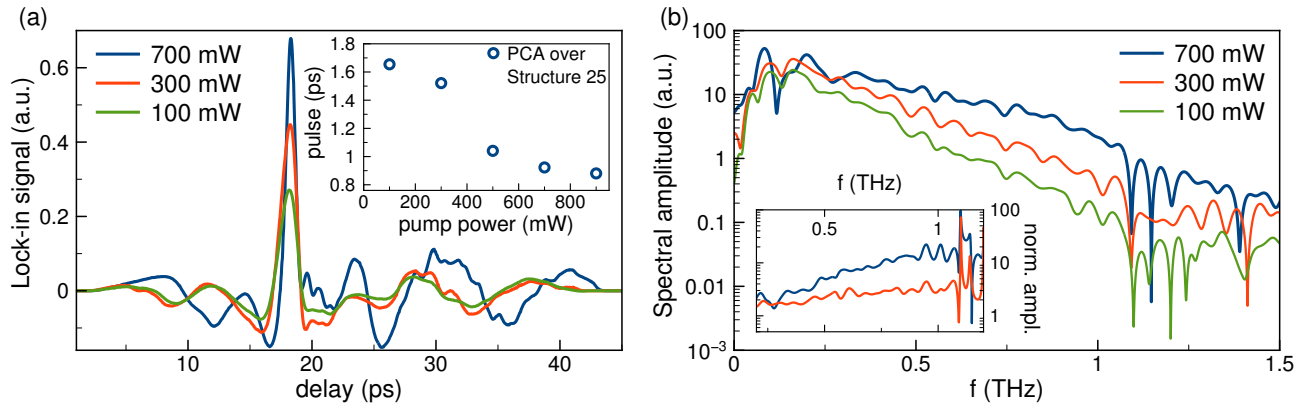


Figure 6. Operation of log-periodic QD Structure 25 PCA under off-resonant high-power pump of 800 nm. (a) Time-domain measurements of the generated THz signal under various pump powers, inset shows dependency of main pulse duration on pump power, (b) Corresponding signal spectra, obtained with Fourier transform from time-domain profiles. Inset shows spectra of 300 mW and 700 mW signals normalised to 100 mW signal spectrum.

THz spectra, in turn acquire stronger higher frequency shoulder, that is clearly seen in Fig. 6 (b). Inset here demonstrates over ten-fold rise of frequency components above 0.6 THz spectral power, and almost no change of signal for components below 0.25 THz, for the same seven-fold pump power change.

Such dependency of generated THz pulse duration and its corresponding spectral width on pump power, also veiledly confirms carrier lifetime shortening under higher pumps described in section 3.

5. QD ANTENNA RESONANT CW OPERATION

Earlier, we have shown very resonant behaviour of QD semiconductor wafers, no matter how they are used, as THz emitter of detector – both generation and sensing efficiency significantly grows when pump wavelength is close to the QD excited state (ES) energy.¹² Such behaviour opens up the possibility to use compact semiconductor ultrafast lasers³ as pump sources, and thus drastically diminish both the dimensions and price of THz tranceiver setup.

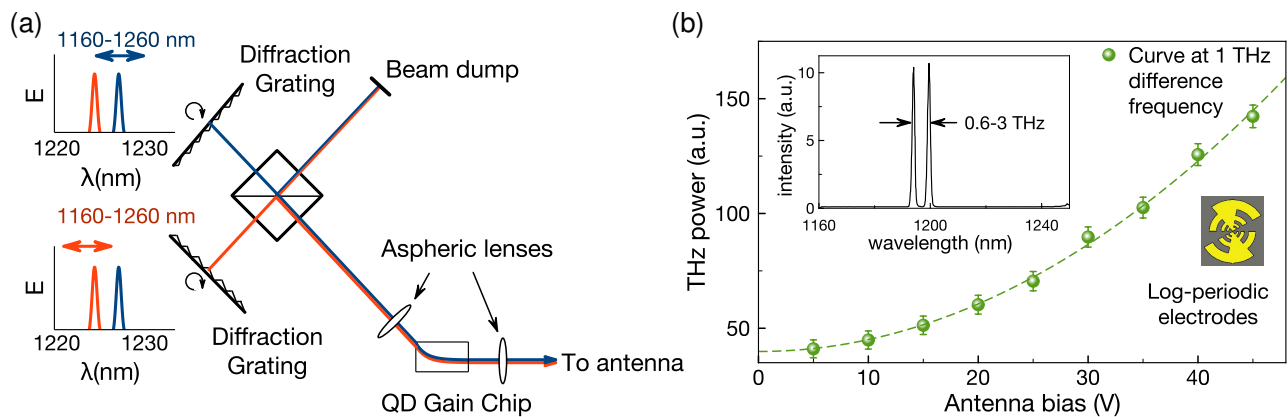


Figure 7. Operation of log-periodic QD-based PCA under resonant pump of compact double-wavelength semiconductor laser. (a) Laser layout scheme, (b) dependence of generated THz power on bias applied to antenna electrodes. Inset: spectrum of the pump laser.

Due to high carrier mobility, not only pulsed THz signals, but also CW THz radiation generation with optimised QD structures is possible and has been demonstrated.^{10,14} For efficient CW THz generation, a proper pump source(s), delivering two closely spaced narrow coherent spectral lines are essential. Double wavelength operation in compact semiconductor lasers can be achieved either by use of Volume Bragg Gratings (VBGs)¹⁰ or double-Littrow configuration cavity, that adds the tunability option.⁴

An example of such CW THz signal obtained with a 5 μm gap log-periodic PCA pumped by double-Littrow configuration laser⁴ tuned to 1 THz difference frequency is shown in Figure 7 (b). Antenna geometry and pump laser optical spectrum are shown in the inset. The THz output power trend is increasing quadratically with PCA bias.

6. OUTLOOK AND PERSPECTIVES

A main goal of the work overviewed in this paper is the development of an ultra-compact, efficient, room-temperature operating THz transceiver system. So far, QD wafers have shown themselves as efficient and perspective materials for both pulsed and CW THz radiation emission. The test structures used for experiments shown here were not optimised, and yet exhibited a signal conversion comparable with state-of-the-art PCA devices. We do expect more tailored QD devices combined with narrow-photogap interdigitated antenna electrodes should allow higher PC gain and generated THz power.

Extremely high thermal tolerance observed allows to propose intracavity antenna placement in, for example, electrically or optically pumped Vertical External Cavity Surface Emitting Laser (VECSEL) (Fig. 8) to exploit the full resonator energy and thus even more enhance conversion efficiency, and, hence, generated THz powers.

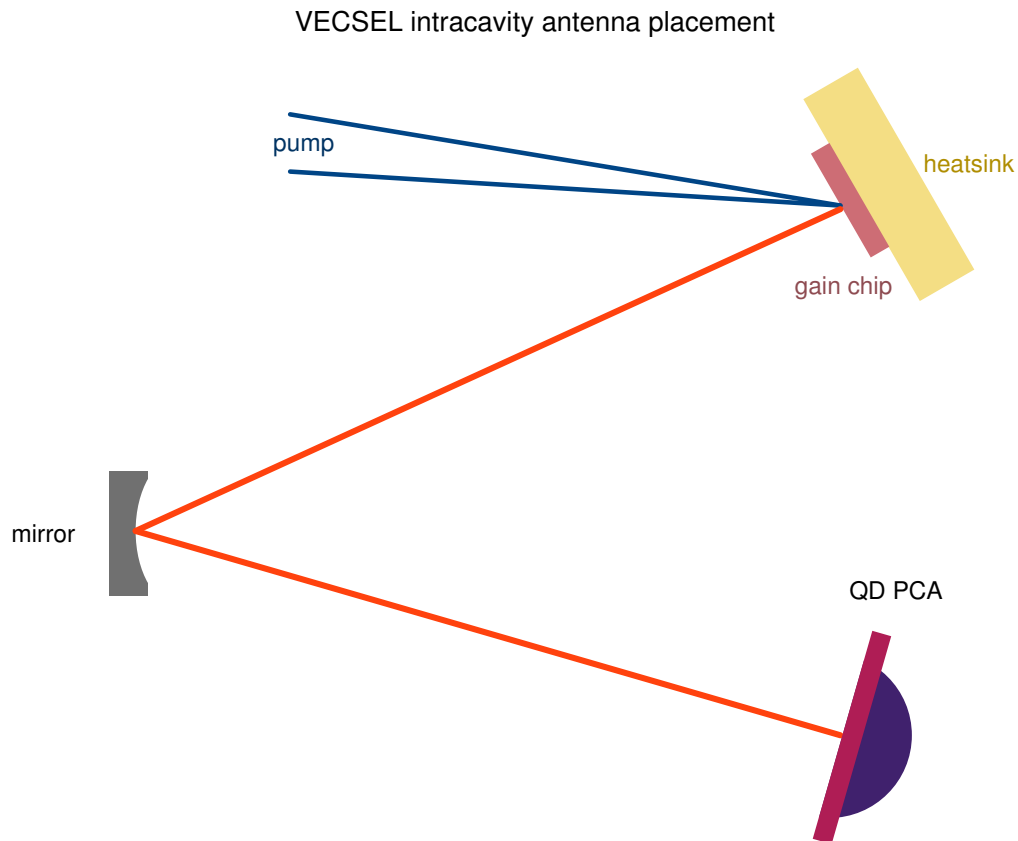


Figure 8. Operation of QD PCA placed inside the cavity of Vertical External Cavity Surface Emitting Laser (VECSEL).

Mutual tunability of the photonic energies of QD LD output signals and QD PCA absorption lines, thermal tolerability of the resulting materials, their ultrafast optoelectronic operation and high carrier mobility foreordain the development of highly configurable compact and easy-to use THz systems. Both the LDs and the PCAs may potentially be fabricated on the same epitaxial semiconductor wafer and thus shrink the device into fully integrated chip.

ACKNOWLEDGMENTS

The authors thank D. Livshits from Innolume GmbH and Edmund Clark of the EPSRC National Centre for III-V Technologies, Sheffield, UK for QD samples growth and Richard Beanland from Integrity Scientific Ltd. for TEM image of a quantum dot. Also, we acknowledge Dr. Ross Leyman, who is currently in Strathclyde University, Glasgow, for pioneering these experiments. This work was supported by EPSRC Grant No EP/H015795/1 and FP7 IAPP TERA project No 285974, sample growth was funded by the NEXPRESSO program. A. G. Thanks Magicplot Ltd. for providing a copy of Magicplot Pro, a cross-platform lightweight app for data analysis, plotting and nonlinear fitting.

REFERENCES

- [1] Auston, D. H., Cheung, K. P., and Smith, P. R., "Picosecond photoconducting hertzian dipoles," *Appl. Phys. Lett.* **45**, 284–286 (1984).
- [2] Ekimov, A. I., Efros, A. L., and Onushchenko, A. A., "Quantum size effect in semiconductor microcrystals," *Solid State Comm.* **56**, 921–924 (1985).
- [3] Rafailov, E. U., Cataluna, M. A., and Sibbett, W., "Mode-locked quantum-dot lasers," *Nat. Photon.* **1**, 395–401 (2007).
- [4] Leyman, R., Nikitichev, D. I., Bazieva, N., and Rafailov, E. U., "Multimodal spectral control of a quantum-dot diode laser for THz difference frequency generation," *Applied Physics Letters* **99**(17), 2011–2014 (2011).
- [5] Wilcox, K., Butkus, M., Farrer, I., Ritchie, D. A., Tropper, A., and Rafailov, E. U., "Subpicosecond quantum dot saturable absorber mode-locked semiconductor disk laser," *Appl. Phys. Lett.* **94**(251105) (2009).
- [6] Rafailov, E. U., Loza-Alvarez, P., Sibbett, W., Sokolovskii, G. S., Livshits, D. A., Zhukov, A. E., and Ustinov, V. M., "Amplification of femtosecond pulses over by 18 db in a quantum-dot semiconductor optical amplifier," *IEEE Photon. Technol. Lett.* **15**, 1023–1025 (2003).
- [7] Rafailov, E. U., White, S. J., Lagatsky, A. A., Miller, A., Sibbett, W., Livshits, D. A., Zhukov, A. E., and Ustinov, V. M., "Fast quantum-dot saturable absorber for passive mode-locking of solid-state lasers," *IEEE Photon. Technol. Lett.* **16**, 2439–2441 (2004).
- [8] Okhotnikov, O., Grudinin, A., and Pessa, M., "Ultra-fast fibre laser systems based on SESAM technology: new horizons and applications," *New Journal of Physics* **6**, 177–177 (nov 2004).
- [9] Tang, M., Minamide, H., Wang, Y., Notake, T., Ohno, S., and Ito, H., "Tunable terahertz-wave generation from DAST crystal pumped by a monolithic dual-wavelength fiber laser," *Optics Express* **19**, 779 (jan 2011).
- [10] Kruczek, T., Leyman, R., Carnegie, D., Bazieva, N., Erbert, G., Schulz, S., Reardon, C., and Rafailov, E. U., "Continuous wave terahertz radiation from an InAs/GaAs quantum-dot photomixer device," *Applied Physics Letters* **101**(8) (2012).
- [11] Leyman, R., Bazieva, N., Kruczek, T., Sokolovskii, G. S., and Rafailov, E. U., "Progress in Compact Room Temperature THz Radiation Sources," *Recent Patents on Signal Processing* **2**, 12–22 (apr 2012).
- [12] Molis, G., Arlauskas, A., Krotkus, A., Leyman, R., Bazieva, N., and Rafailov, E., "THz emission spectroscopy of self-organized InAs quantum dot ensembles," in [*2012 37th International Conference on Infrared, Millimeter, and Terahertz Waves*], 1–2, IEEE (sep 2012).
- [13] Leyman, R., Carnegie, D., Bazieva, N., Molis, G., Arlauskas, A., Krotkus, A., Schulz, S., Reardon, C., Clarke, E., and Rafailov, E. U., "Characterisation of InAs:GaAs quantum dot-based photoconductive THz antennas," in [*2013 IEEE Photonics Conference*], **4**, 418–419, IEEE (sep 2013).
- [14] Rafailov, E. U., Leyman, R., Carnegie, D., and Bazieva, N., "Highly efficient quantum dot-based photoconductive THz materials and devices," **8846**, 88460I (sep 2013).

- [15] Gorodetsky, A., Rafailov, E. U., and Leyman, R., “Quantum Dot-Based Terahertz photoconductive antennas,” in [2014 *International Conference Laser Optics*], **94**, 1–1, IEEE (jun 2014).
- [16] Leite, I. T., Gorodetsky, A., Leyman, R., Bazieva, N., and Rafailov, E. U., “Towards High-intensity Terahertz Generation : InAs / GaAs Quantum Dots Based Antennae Optically Pumped Up To 1 W,” in [2015 *Conference on Lasers & Electro-Optics Europe & International Quantum Electronics Conference CLEO EUROPE - EQEC*], **105**(2007), 81114 (2015).
- [17] Malins, D. B., Gomez-Iglesias, A., White, S. J., Sibbett, W., Miller, A., and Rafailov, E. U., “Ultrafast electroabsorption dynamics in an InAs quantum dot saturable absorber at 1.3 μm ,” *Applied Physics Letters* **89**(17), 171111 (2006).
- [18] Lumb, M. P., Clarke, E., Harbord, E., Spencer, P., Murray, R., Masia, F., Borri, P., Langbein, W., Leburn, C., C. Jappy, N., Metzger, Brown, C., and Sibbett, W., “Ultrafast absorption recovery dynamics of 1300 nm quantum dot saturable absorber mirrors,” *Appl. Phys. Lett.* **95**, 041101 (2009).
- [19] Hoffmann, M. C., Monozon, B. S., Livshits, D., Rafailov, E. U., and Turchinovich, D., “Terahertz electroabsorption effect enabling femtosecond all-optical switching in semiconductor quantum dots,” *Applied Physics Letters* **97**(23), 231108 (2010).
- [20] Gorodetsky, A., Leite, I. T., Bazieva, N., and Rafailov, E. U., “Optical Pump Terahertz Probe Carrier Lifetime Measurement in InAs / GaAs Quantum Dots Based Photoconductive Antennae,” in [2015 *Conference on Lasers & Electro-Optics Europe & International Quantum Electronics Conference CLEO EUROPE - EQEC*], **2441**(2013), 88460 (2015).
- [21] Borri, P., Schneider, S., Langbein, W., and Bimberg, D., “Ultrafast carrier dynamics in InGaAs quantum dot materials and devices,” *Journal of Optics A: Pure and Applied Optics* **8**, S33–S46 (apr 2006).
- [22] “Batop GmbH. PCA - photoconductive antenna for THz waves.” www.batop.com/products/terahertz/photoconductive-antenna/photoconductive-terahertz-antenna.html. (Accessed: 20 January 2016).
- [23] “Teravil Ltd. Free space THz Detector.” www.teravil.lt/detector.php. (Accessed: 20 January 2016).